

Figures

Figure 19 (cover of chapter II on page 90): Ribosomes in the asymmetric unit

One asymmetric unit contained 2 copies of the ribosome that are positioned in the crystal lattice as shown here.

The 30S and 50S subunit of the first ribosome (70S #1) are shown in yellow and magenta, respectively. In case of the second ribosome (70S #2) the 30S is colored in cyan whereas the 50S is shown in white.

Figure 20: Ratchet-linker model (Frank and Agrawal 2000)

The 30S and 50S subunit are shown in yellow and blue respectively. Elongation factors G (EF-G) is shown in red. An anticlockwise movement of the 30S subunit with respect to the 50S subunit, shown by the black arrow, upon binding of EF-G (**B**) has been observed by a cryo-EM reconstruction by the Frank group.

A 70S/fMet tRNA^{fMet} complex

B 70S/EF-G/GMPPNP complex

The Figure was taken out of (Frank and Agrawal 2000)

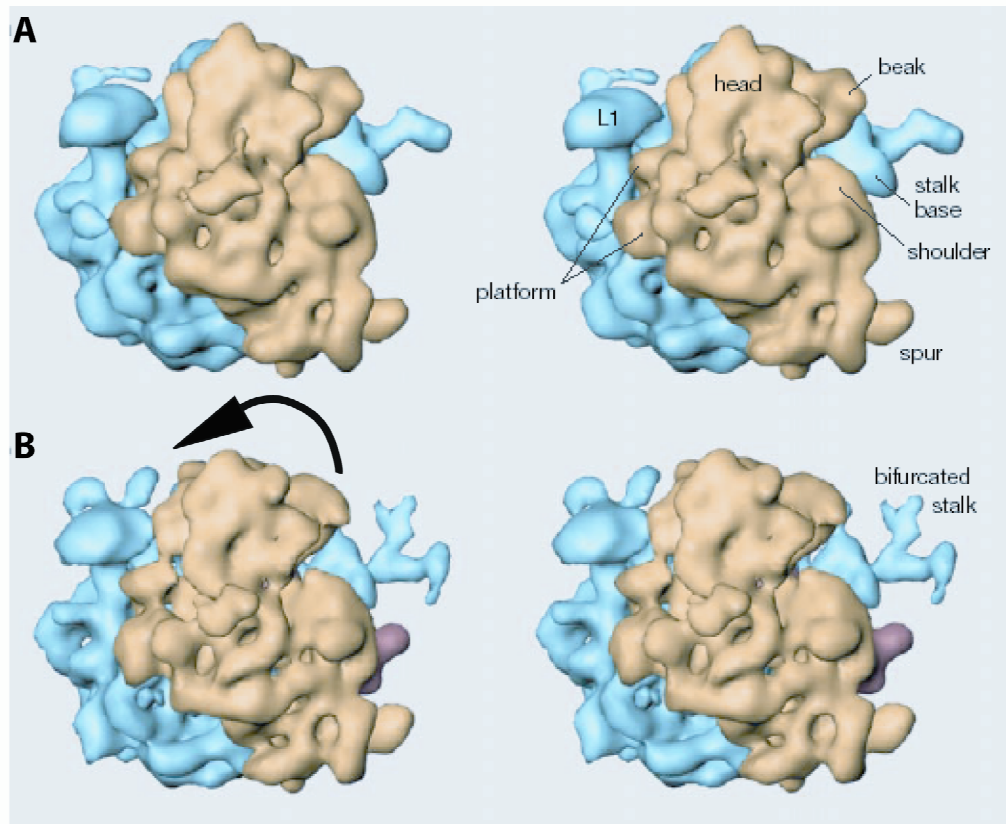
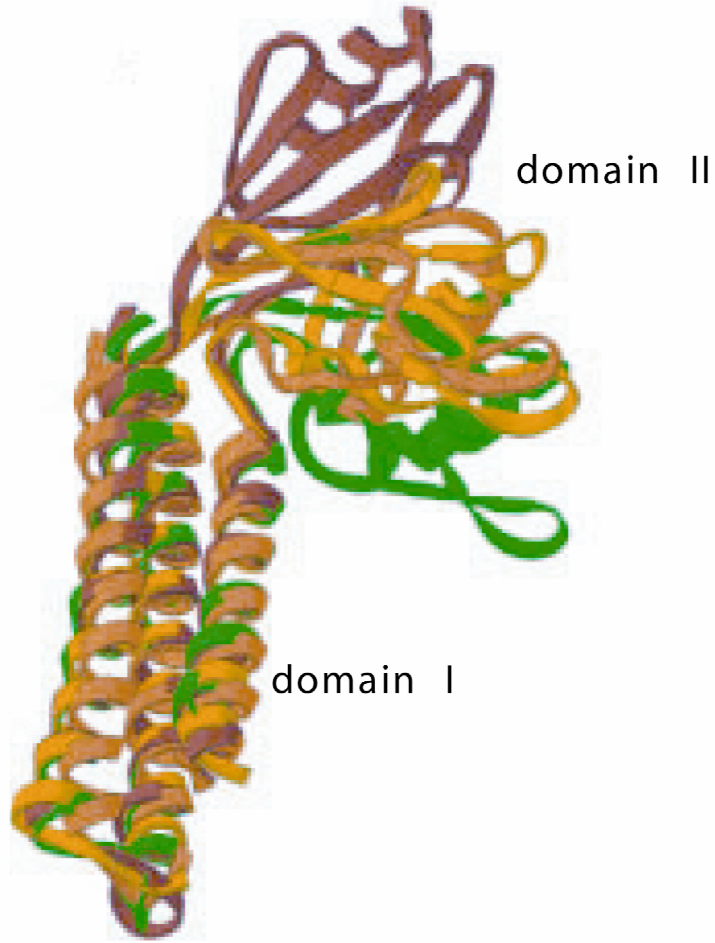


Figure 21: X-ray structures of the Ribosome Recycling Factor

A Superposition of domain I of RRF from *T. maritima* (Selmer, Al-Karadaghi et al. 1999) (green), *T. thermophilus* (Toyoda, Tin et al. 2000) (yellow), *A. aeolicus* (Yoshida, Uchiyama et al. 2001) (orange), and *E. coli* (Kim, Min et al. 2000) (red). The Figure was taken from (Lancaster, Kiel et al. 2002).

B Superposition of RRF structure (shown in blue) and yeast tRNAPhe (shown in red) suggest a molecular mimic. The Figure is taken from (Selmer, Al-Karadaghi et al. 1999)

A



B

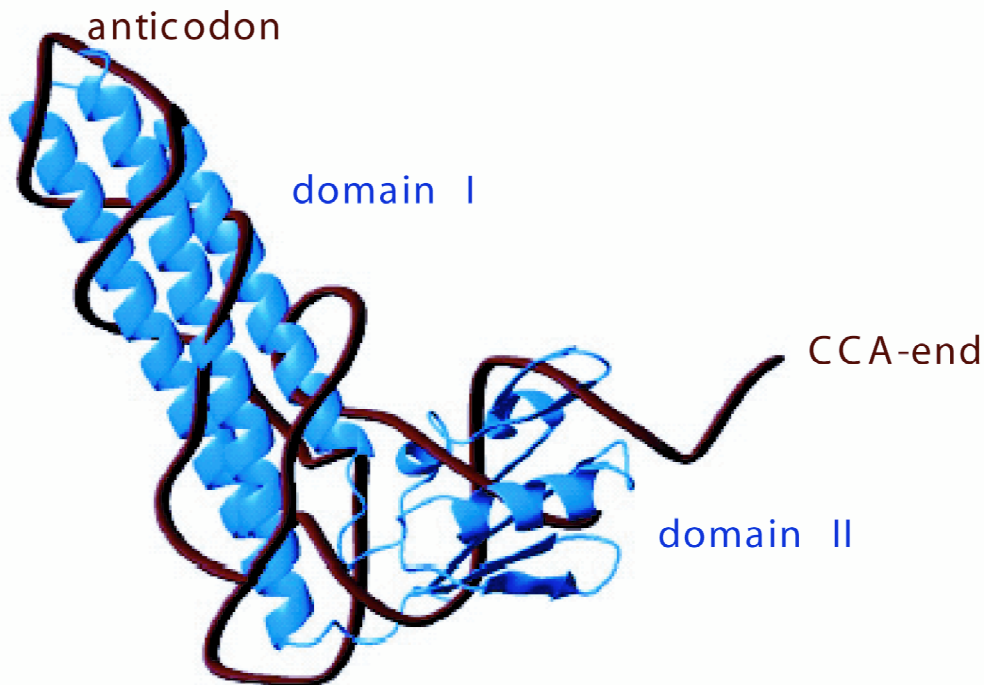


Figure 22: S1 content

A OD₂₆₀ spectrum of ribosomal subunits treated with Poly-U after sucrose gradients. The first peak contains a mixture of Poly-U and S1, followed by a 30S and a 50S peak

B SDS page of (lane 1) Poly-U/S1 peak from A and (lane 2) and 70S-R preparation depleted of S1 by Poly-U treatment.

C 70S (tight coupled) run on a composite gel separate three different forms for 50S (50S, containing all the proteins, 50S-M lacking L7/L12, 50S-F lacking L7/L12/L11/L10) and two different forms for the 30S subunit (30S, containing all the proteins, 30S-F lacking S1).

D Analysis of different ribosome preparations on composite gel: 10 µg of 70S-tight coupled were loaded on lane 1, 10 µg and 20µg of 70S-R were loaded on lane 2 and 3, respectively.

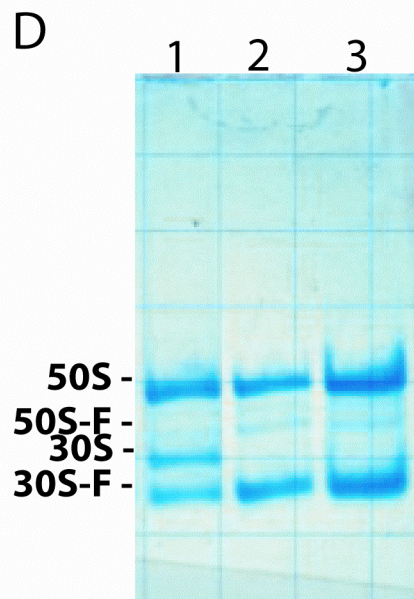
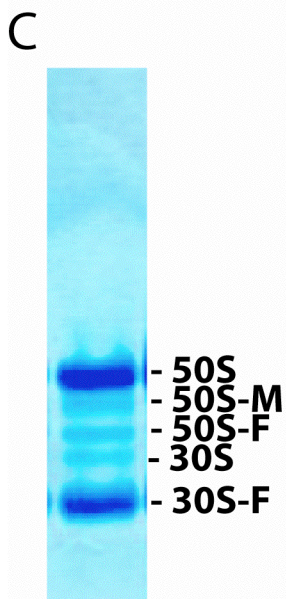
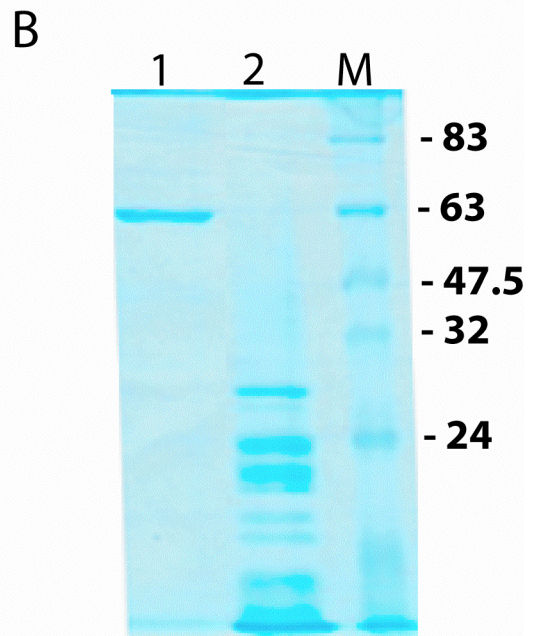
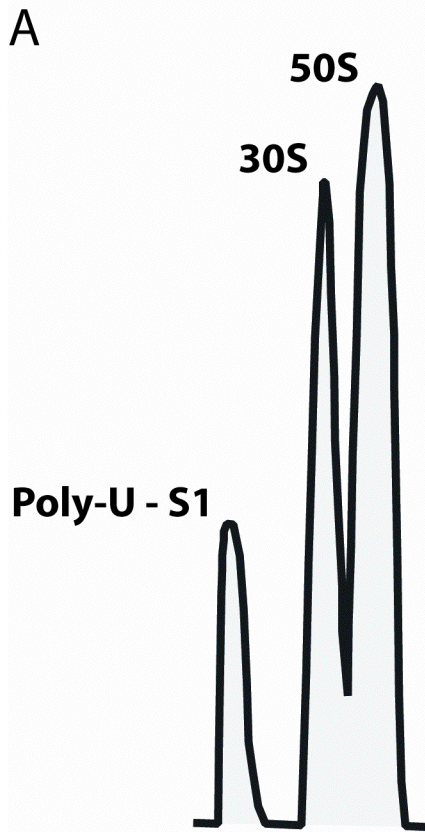


Figure 23: P2₁2₁2₁ crystals of 70S *E. coli* ribosomes

Crystals of the 70S *E. coli* ribosome were grown using the micro-batch method resulting in different sizes dependent of the growth time. The ruler ranges from 0 to 500 μm .

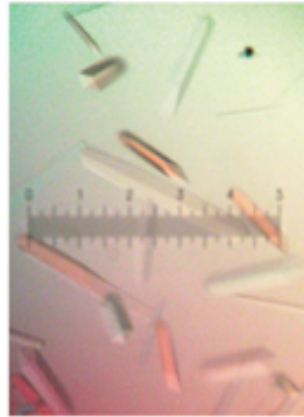
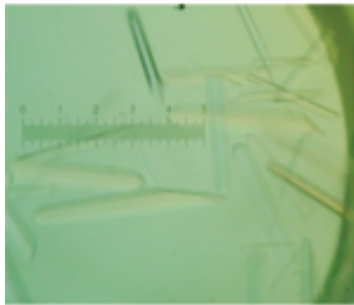
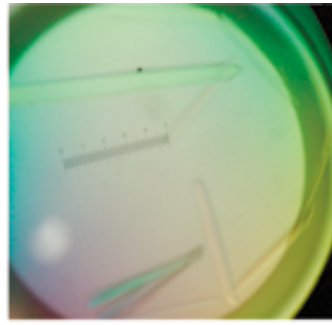


Figure 24: Mounting of the crystals

A The crystals had to be mounted in a way that they would stick out of the loop. The Figure shows a crystal in the beam. The dimensions of the Figure are about 200 μm x 200 μm . The crystal itself has a length of 100 μm on its shortest axis.

B +C Difference between non-bendable (**B**) and bendable loops (**C**) (Hampton Research). The latter had to be bended in a specific way, shown at the bottom of the C in order for the crystal to rotate 360°.

D Output of the program written by James' Holton (scientist at beamline 8.3.1 at the Advanced Light Source). The amount of missing reflections are shown at the y-axis (hkl in %), the corresponding phi angles are shown at the x-axis, ranging from 0-180°.

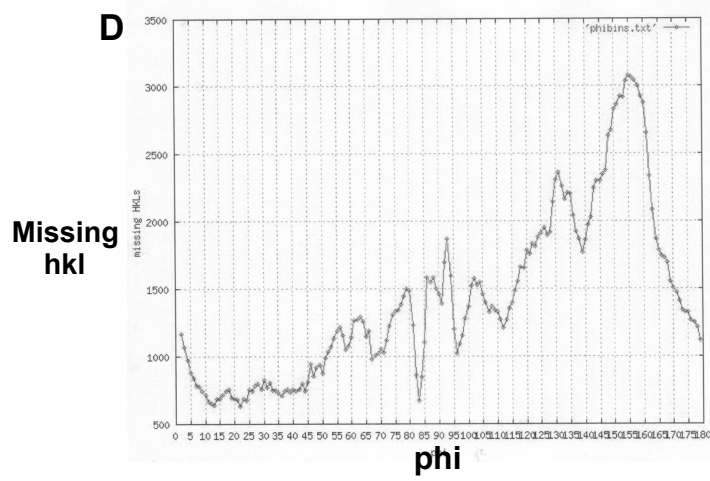
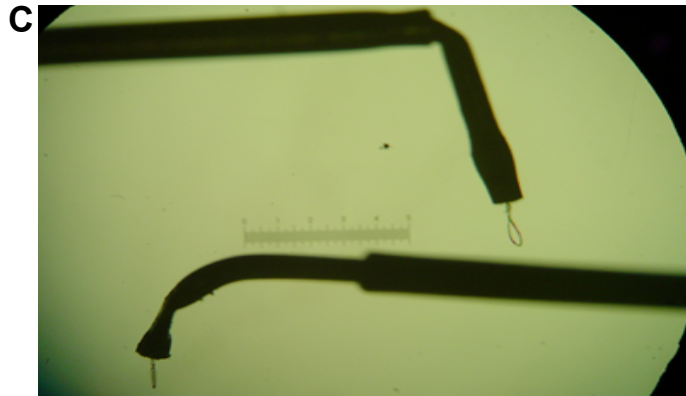
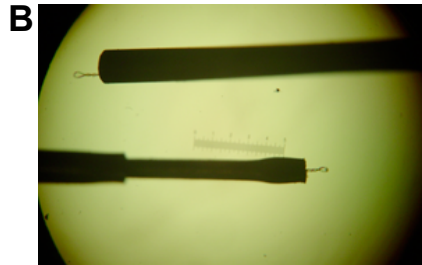
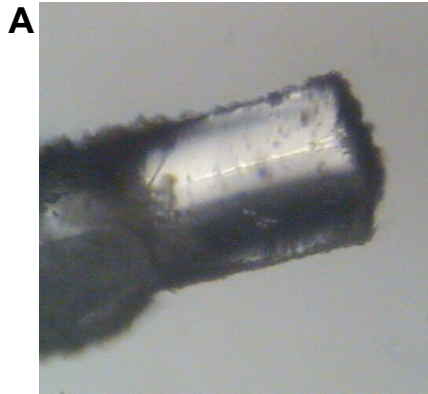
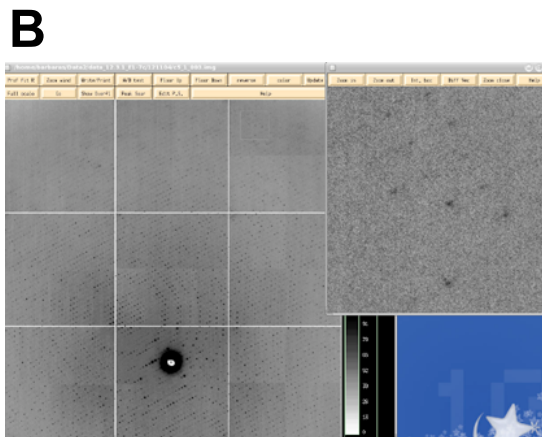
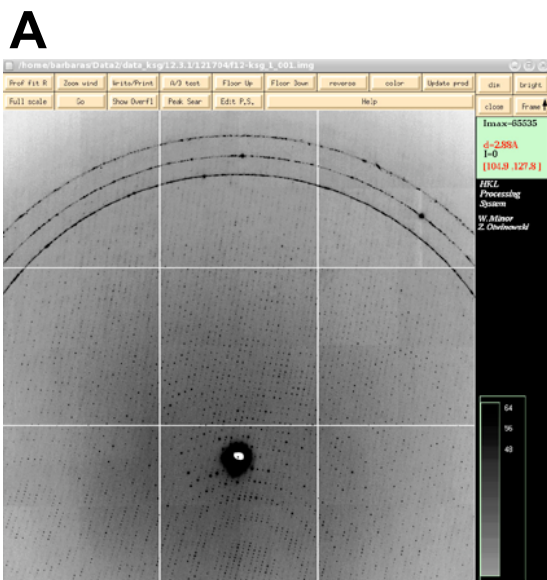


Figure 25: Icerings

A Example for strong icerings that were present on the diffraction pattern of the P212121 crystals.

B One was able to remove most of the ice by washing the crystal resulting in weak icerings on the diffraction pattern.

C Output (log file) of the final scalepack file after several rounds of rejection that was used for the calculation of electron density maps. Chi2 values in the icering regions are pointed out.



C

Shell	Lower	Upper	Average	Average	Norm. Linear	Square	
limit	Angstrom	I	error	stat.	Chi**2	R-fac	R-fac
200.00	11.73	7820.2	426.9	49.6	1.023	0.071	0.08
.
.
4.01	3.96	796.2	153.3	118.3	1.001	0.269	0.261
3.96	3.91	758.3	181.9	146.5	1.183	0.306	0.303
3.91	3.86	728.5	192.8	159.6	1.364	0.338	0.323
3.86	3.82	830.6	220.5	186.2	1.601	0.372	0.364
3.82	3.78	658.7	190.7	163.5	1.203	0.363	0.357
3.78	3.73	627.1	193.8	168.5	1.191	0.377	0.374
3.73	3.69	608.6	195.1	170.9	1.157	0.390	0.379
3.69	3.66	576.3	199.2	177.0	1.153	0.412	0.402
3.66	3.62	589.8	216.2	194.2	1.478	0.483	0.482
3.62	3.59	553.9	214.6	197.1	1.225	0.526	0.503
3.59	3.55	488.1	203.4	186.7	1.099	0.496	0.488
3.55	3.52	461.1	205.1	190.1	1.111	0.531	0.522
3.52	3.49	444.2	211.5	197.4	1.107	0.561	0.547
3.49	3.46	422.6	213.1	200.5	1.089	0.595	0.581
3.46	3.43	397.1	216.6	204.8	1.106	0.632	0.610
All reflections		1358.5	183.9	108.7	1.033	0.145	0.119

Figure 26: Secondary structures of 5' half of the 23S rRNA

Secondary structures of **A**, *Escherichia coli*, **B**, *Deinococcus radiodurans* and **C**, *Haloarcula marismortui* were taken from Robin Gutell's website (Gutell).

Blow-up of domain I of the 23S rRNA in the case of **A** and **B** show a far more extended helix in the case of *E. coli* (**A**) than in the case of *D. radiodurans* (**B**) used as an example for an insertion (red arrows).

Blow-up of domain I reveals a conserved region between *E. coli* (**A**) and *H. marismortui* (**C**) pointed out with the help of a green arrow.

Figure 27: Restraints used in the refinement process

Figures A and B were taken from “Principles of Nucleic Acid Structure” by Wolfram Saenger.

A 28 possible base-pairs between A, G, U (T) and C within nucleic acids were defined in the Saenger-classifications.

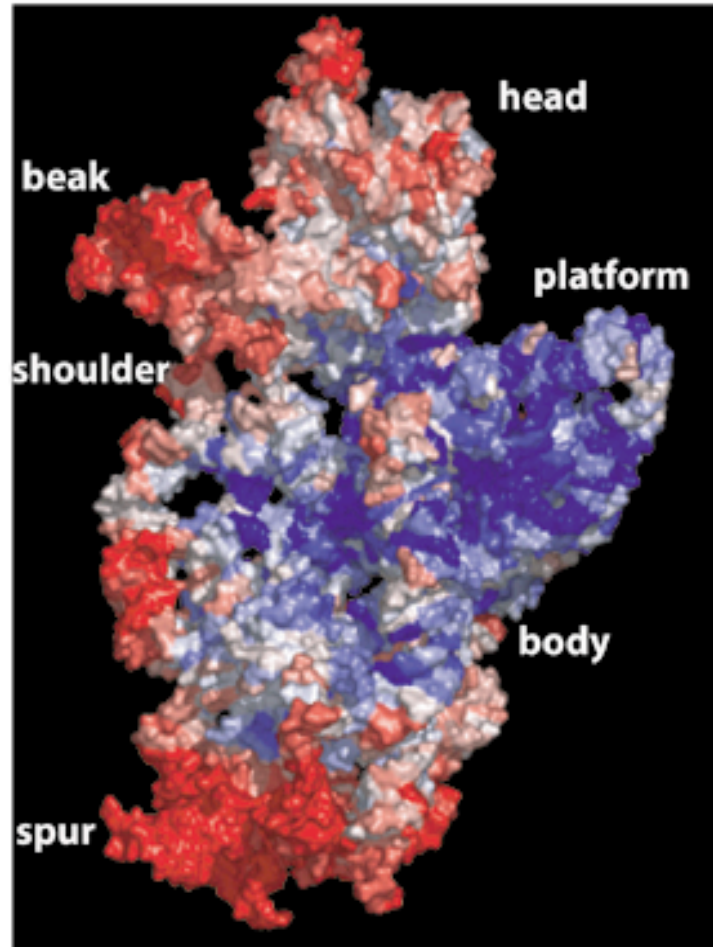
B Definition of the six torsion angles (α , β , γ , δ , σ , ϵ) and the atomic numbering scheme within nucleic acid chains.

Figure 28: B-factor diagram of the small 30S subunit

B-factors ranging from 0-50 Å² are shown in blue, from 50-100 Å² in white and regions containing high b-factors (100-150 Å²) are highlighted in red. The different regions of the 30S subunit are marked as head, platform, body, spur, shoulder and beak.

B-factors of the 16S rRNA are shown from the intersubunit space in **A** and from the solvent site in **B**.

A



B

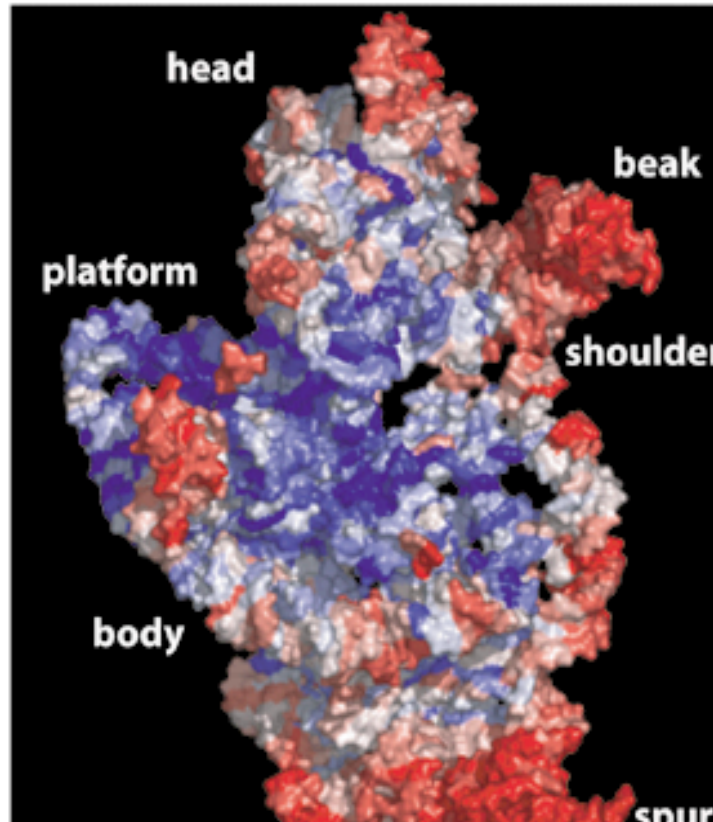


Figure 29: B-factor diagram of the small 50S subunit

B-factors ranging from 0-50 Å² are shown in blue, from 50-100 Å² in white and regions containing high b-factors (100-150 Å²) are highlighted in red. The different regions of the 50S subunit are marked as L1, L7/L12 (making up the stalk), CP (Central protuberance) and the region of the 5S rRNA all characterizing the crown-shape of the large subunit.

B-factors of the 23S rRNA are shown from the intersubunit space in **A** and from the solvent site in **B**.

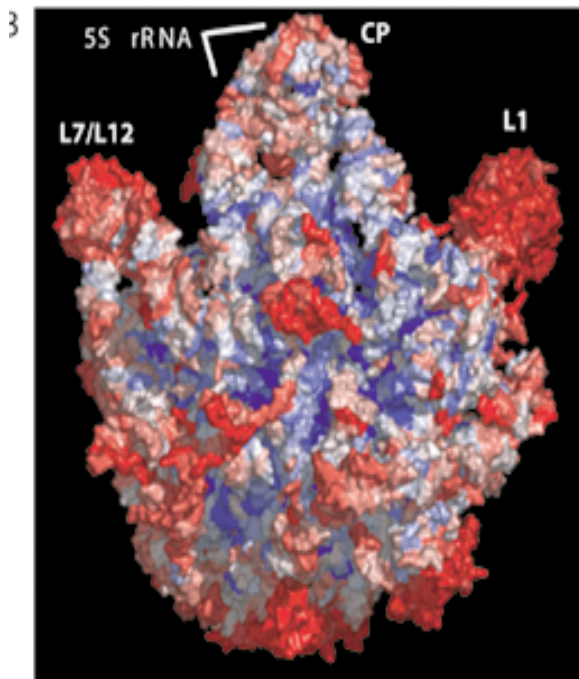
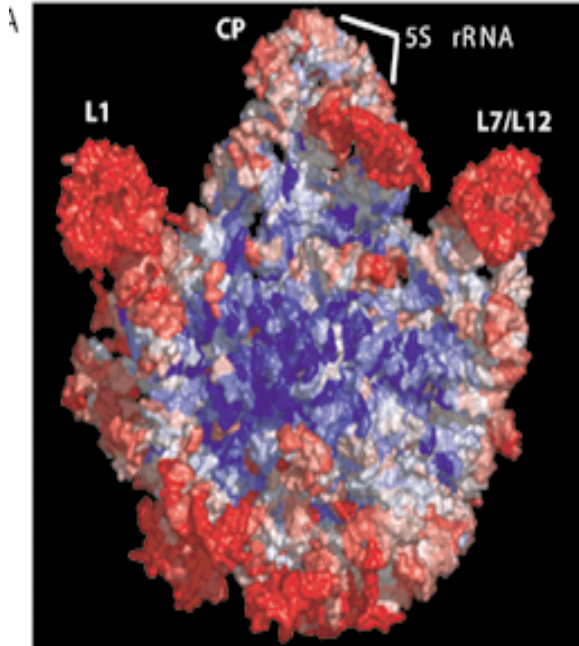
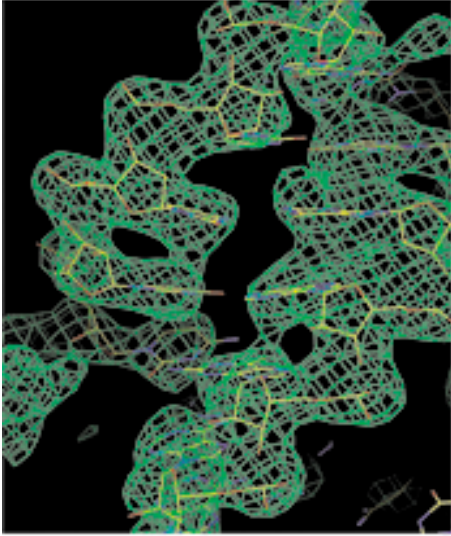


Figure 30: Electron density map

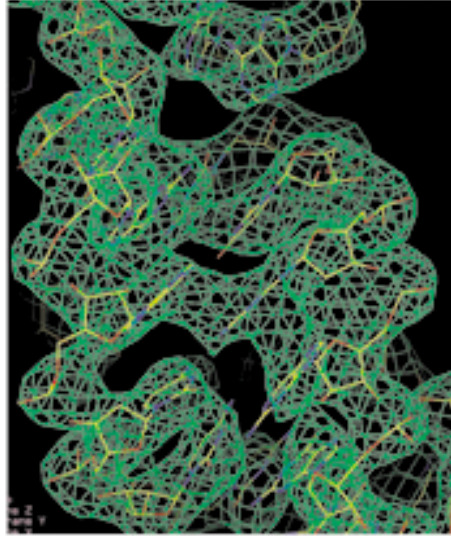
Fitting of different regions of the ribosome model into the $3F_{\text{obs}}-2F_{\text{calc}}$ maps (green density) are shown in **A**, **B** and **C**. The threshold in A and B is set to $\sigma = 2$. At $\sigma = 2.5$ (**C**) one is able to distinguish between pyrimidines and purines.

D Positive density (blue) for magnesium ions was observed in a $F_{\text{obs}} - F_{\text{calc}}$ map. The magnesium ions are coordinated by the phosphate groups (red in the model) surrounding them. The threshold level was set to $\sigma = 5$.

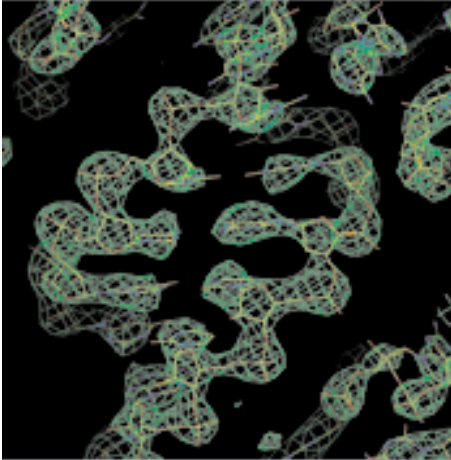
A



B



C



D

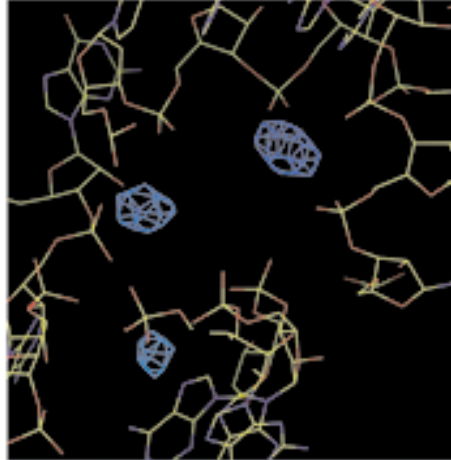


Figure 31: Movement of the 30S subunit

The 30S subunits are shown from the subunit interface, the head is tilted towards the 50S subunit. Regions of the 30S subunit are marked as H (head), B (beak) and S (spur). In addition, the relative position of the three tRNA binding sites is shown as A (site), P (site) and E (site).

Superposition of the two 16S rRNA (30S subunits) (molecule #1 is shown in magenta, molecule #2 in yellow) of the two 70S molecules (#1 and #2) reveal a movement in the head and beak region that follows a half circle (yellow arrow on the top) towards the 50S subunit. The spur region was observed to move upwards at the same time (yellow arrow on the bottom). The movement in Angstrom (Å) within the different regions is shown.

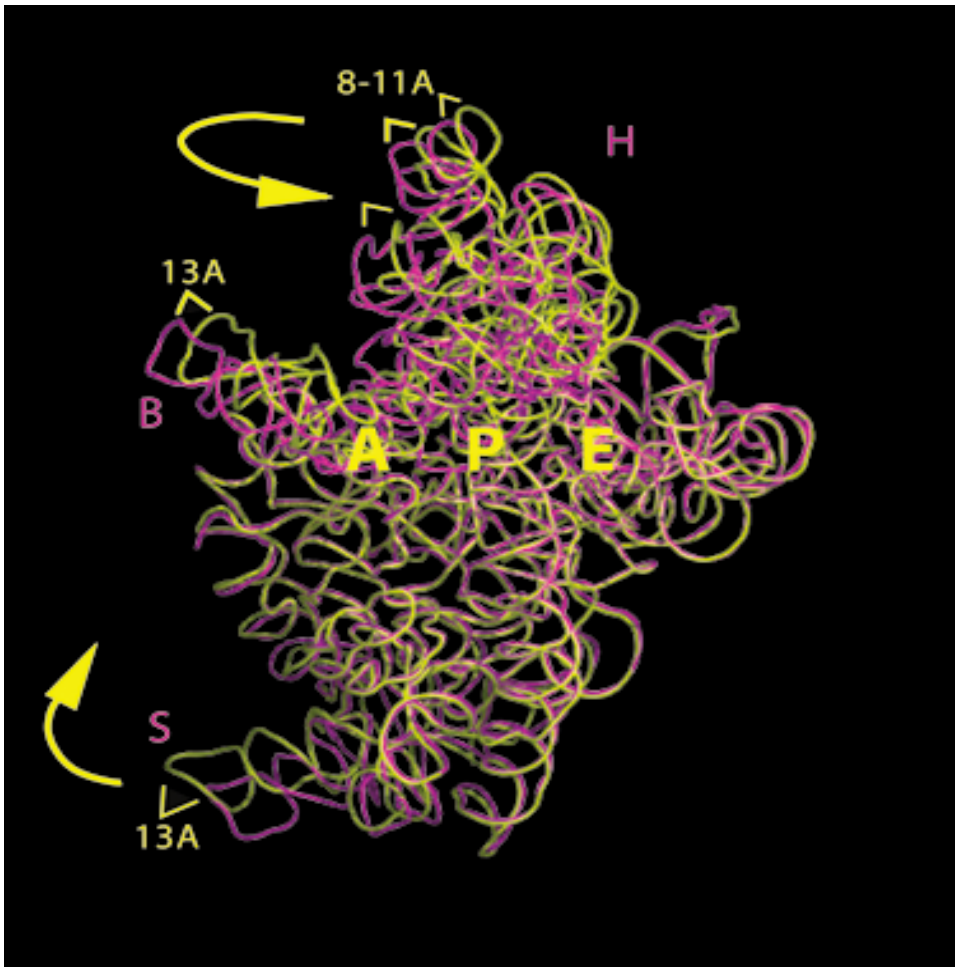


Figure 32: Movement of the 50S subunit

Superposition of the rRNA (23S and 5S) of the 50S subunits (molecule #1 is shown in magenta, molecule #2 in yellow) of the two 70S molecules (#1 and #2) reveal a movement (in Angstrom) within the L1 (moving away from the CP) and L7/L12 region (moving towards the subunit cavity)

The 50S subunits are shown from the intersubunit space. The regions that characterize the crown-shape of the large subunit are marked as L1, CP (Central protuberance) and L7/L12. The position of A-, P- and E-site is shown as yellow A, P, E.

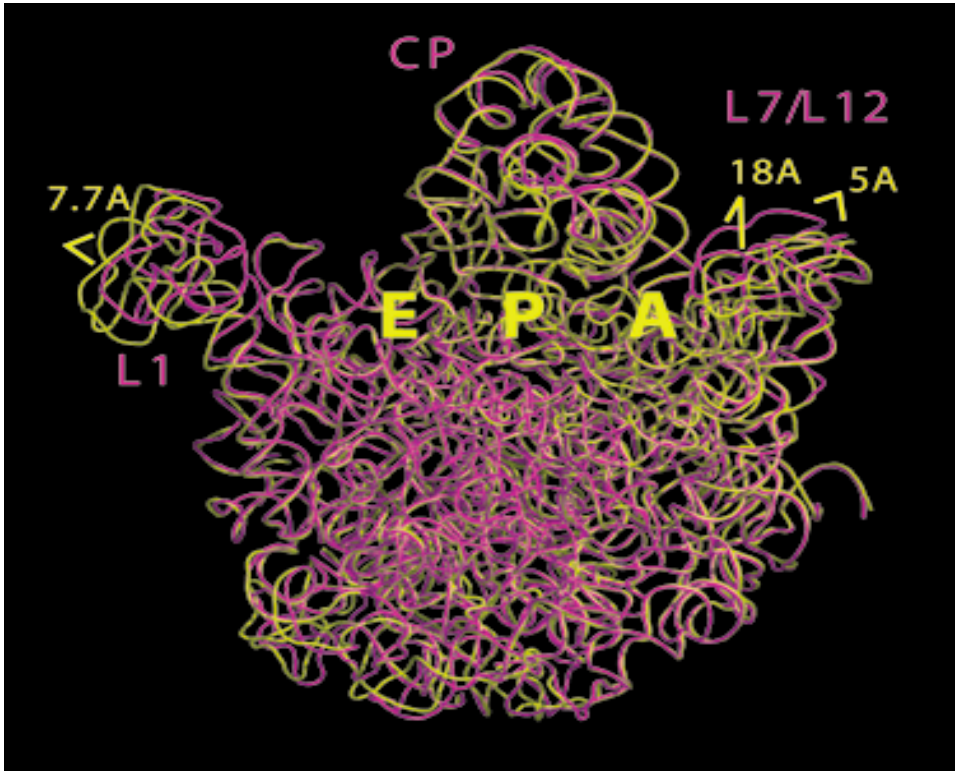


Figure 33: Movement of the subunits with respect to each other

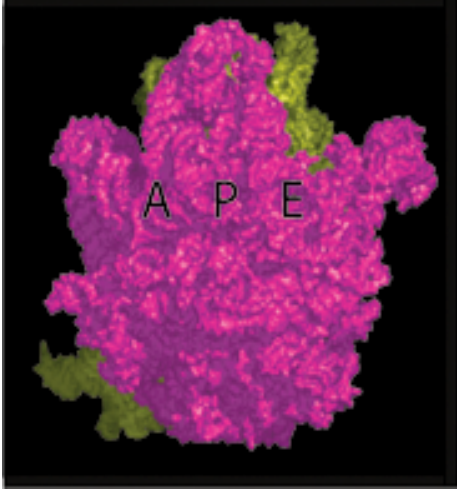
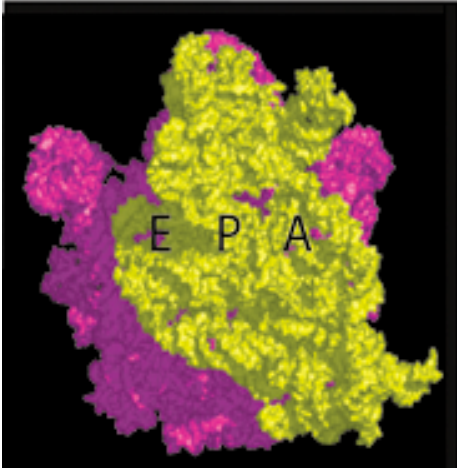
5S rRNA and 23S rRNA of the 50S are shown in magenta, 16S rRNA of the 30S is shown in yellow. The three tRNA binding sites are marked as A, P and E. In both parts of the figure, **A** and **B**, the top part represents the view from the solvent site of the small 30S subunit and the bottom part the view from the solvent site of the large 50S subunit.

A Position of the two subunits relative to each other in 70S molecule #1.

B Position of the two subunits relative to each other in 70S molecule #2.

The movement occurring in molecule #2 with respect to molecule #1 is indicated with the help of yellow arrows.

A



B

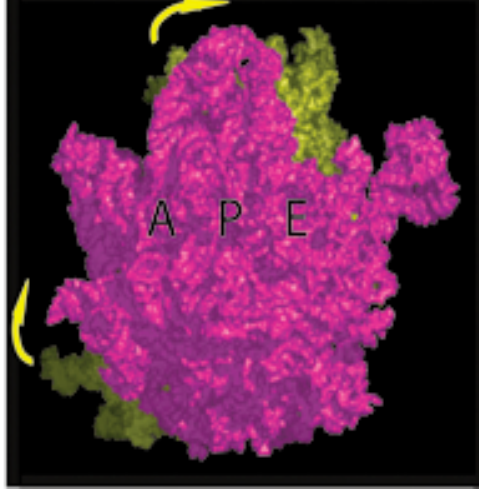
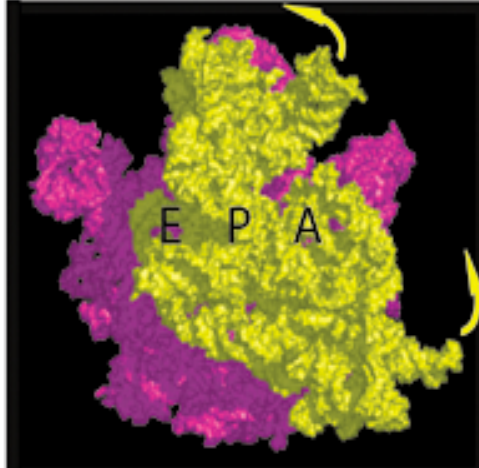


Figure 34: Kasugamycin

A Chemical formula of the aminoglycoside kasugamycin

B $F_{\text{obs}} - F_{\text{calc}}$ map at 3.5 Å resolution (60% complete) reveal a blob of positive density at the 30S subunit. Positive and negative density are shown in blue and red, respectively. The 16S rRNA and the proteins of the 30S subunit are colored in magenta.

C + D Blow up of the kasugamycin binding site in molecule #1 (**C**) and in molecule #2 (**D**) of the two 70S molecules within the asymmetric unit. Positive density (blue) that can be attributed to kasugamycin was found between G926 and A794 of the 16S rRNA. The 16S rRNA of molecule #1 and molecule #2 is colored in magenta and yellow, respectively.

The threshold for the density was set to $\sigma = 3$.

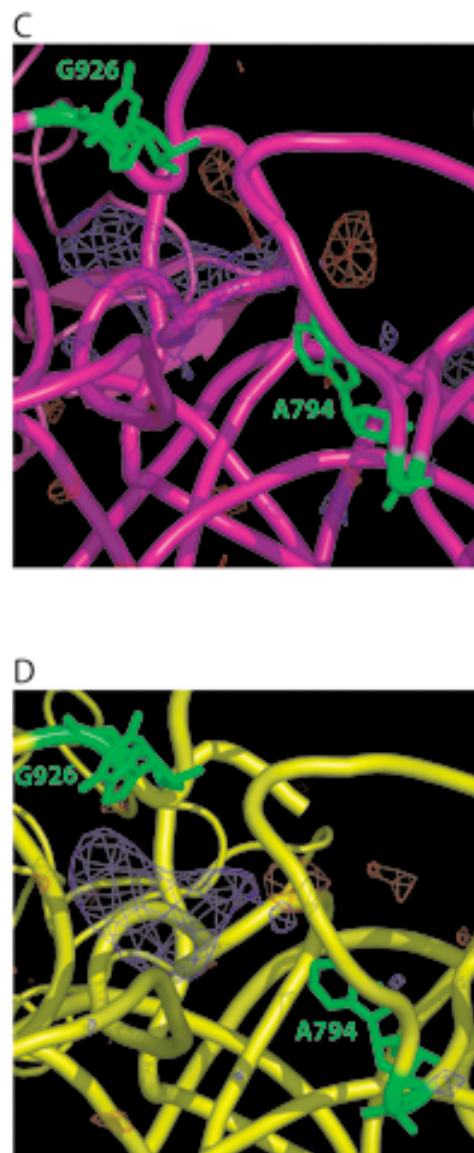
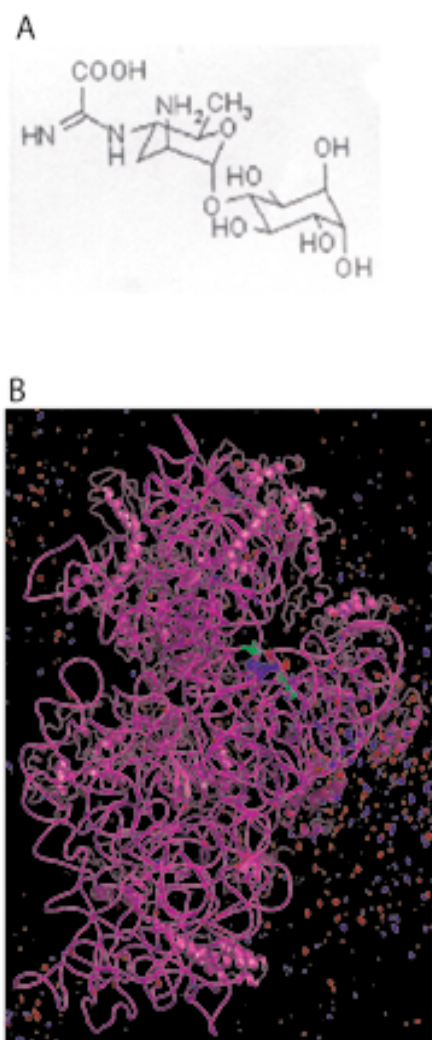


Figure 35: Ribosome Recycling Factor (RRF)

RRF was successfully soaked into the new crystal form. However, positive density that can be attributed to domain I of the factor was only observed in molecule #2. The $F_{\text{obs}} - F_{\text{obs}}$ map was done with a dataset to 8Å resolution. The threshold was set to $\sigma = 2.8$. The 23S rRNA is colored in magenta, helix 69 is labeled.

A Binding site of ecRRF with respect to the complete *E. coli* 70S ribosome (molecule #2). The 30S subunit is shown in cyan, the 50S subunit in magenta, RRF in yellow and its positive density is shown in blue.

B Binding site of ecRRF (yellow) on the 50S subunit (magenta) looking onto the subunit interface. Positive and negative density are shown in blue and red respectively.

C Blow-up of the ecRRF binding site between G2253, C1947 and m_1915. Positive density (blue) was only observed for domain I of the factor whereas the one for domain II is missing. Domain I of *E. coli* RRF has been docked into the density.

D Superposition of the observed positive and negative densities from 8Å $F_{\text{obs}} - F_{\text{obs}}$ maps of soaking experiments using ecRRF or ttRRF. In case of the ecRRF positive and negative density are shown in green and yellow, respectively. In the case of ttRRF the positive density is shown in blue, the negative density is shown in red.

The X-ray structure of ecRRF (shown in yellow) (Kim, Min et al. 2000) has been used.

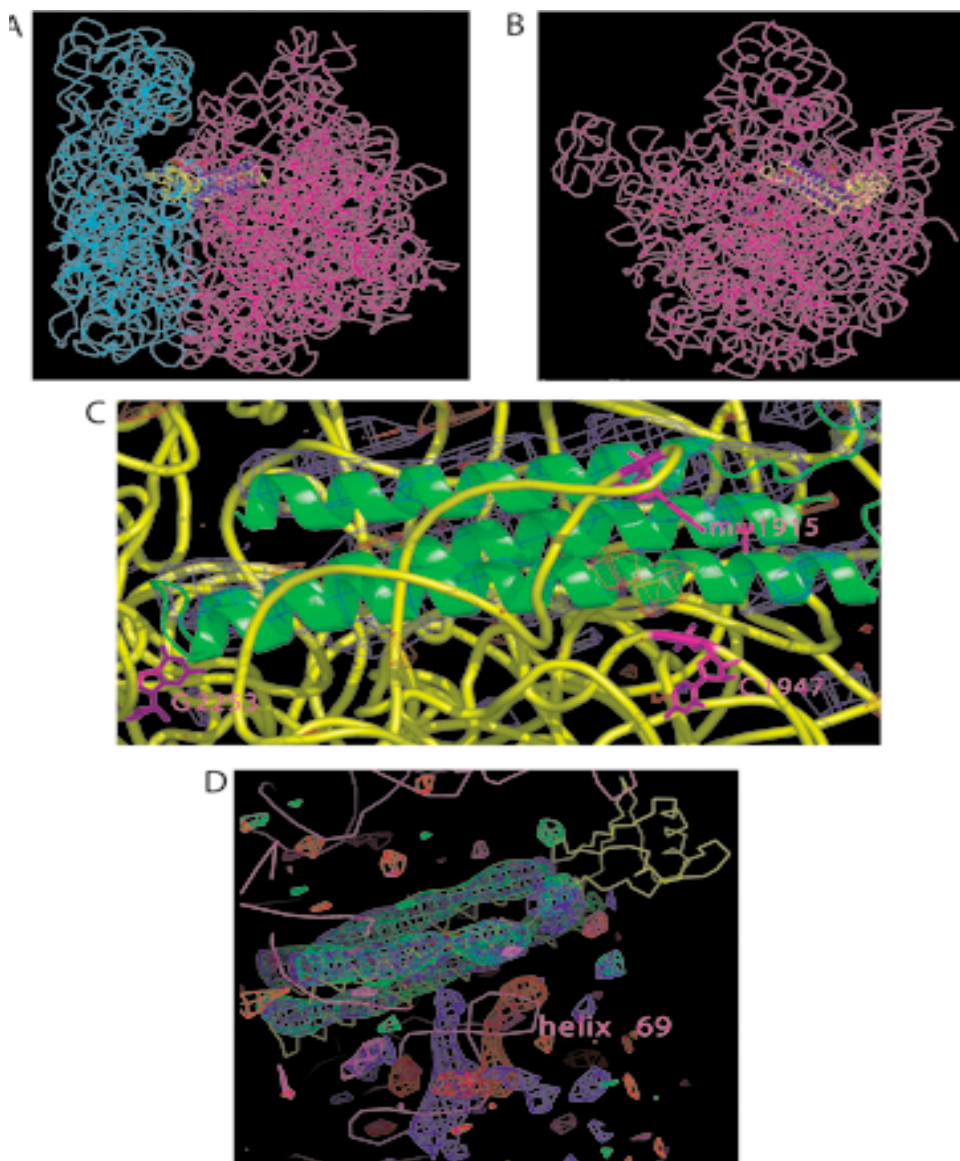
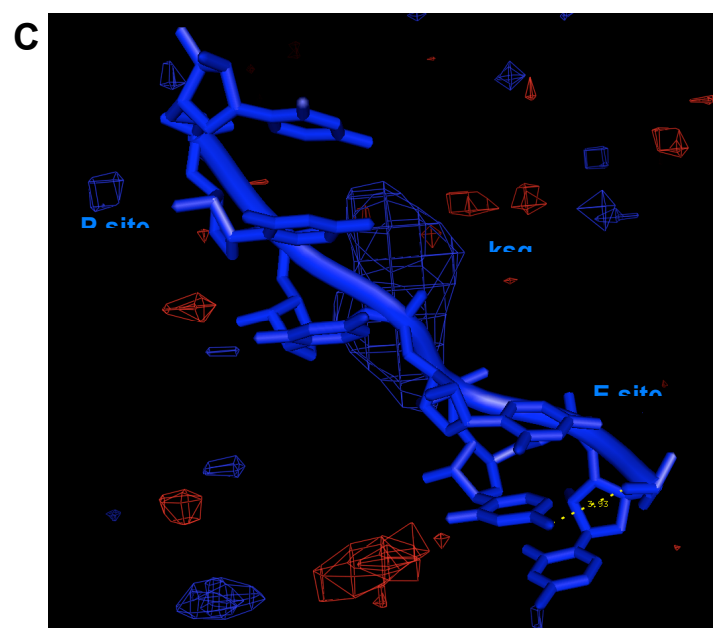
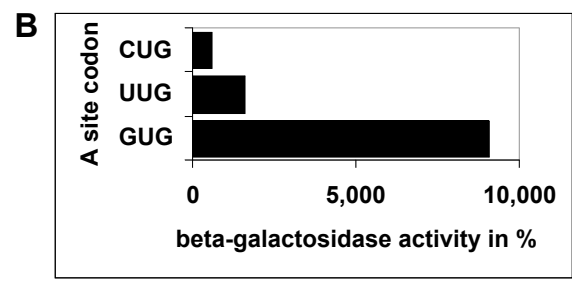
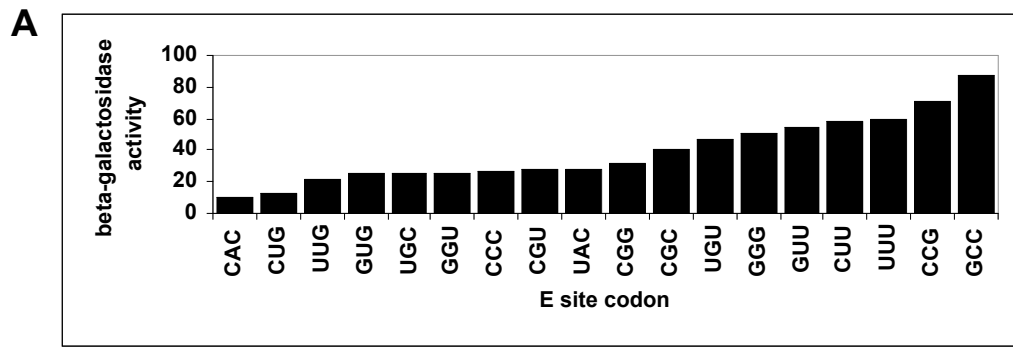


Figure 36: Inhibition by kasugamycin

A mRNA constructs with different sequences at the E site codon, but with the same P site codon (AUG), have been used to investigate the inhibitory effect of kasugamycin on translation initiation by means of β -galactosidase assays. The E site mutations are shown at the x-axis of the figure. The y axis shows the relative amount of β -galactosidase produced in the presence of kasugamycin in %. The data has been observed by J. M. Day (Day).

B Inhibitory effect of kasugamycin with a 'CCC' codon at the E site using different start codons by means of β -galactosidase assays. The different start codons at the P site are shown at the axis. The y axis shows the relative amount of β -galactosidase produced in the presence of kasugamycin in %. The data has been observed by J. M. Day (Day).

C Kasugamycin overlaps the path of the mRNA. The $F_{obs}-F_{obs}$ electron density map of kasugamycin has been superimposed onto the 3' end of the 16S rRNA that folds back into the mRNA channel, thereby mimicking an mRNA. The 'mRNA' was used from the 30S structure by the Ramakrishnan group {Wimberly, 2000 #343}. A potential hydrogen bond between cytosine at the second position of the E site codon with the phosphate group of the cytosine at the third position of the E site codon is indicated by the dashed yellow line.



Tables

Table 3: Diffraction statistics for the *E.coli* 70S ribosome crystals

	Apo 70S	70S-ksg complex
Data collection		
Space group	P2 ₁ 2 ₁ 2 ₁	P2 ₁ 2 ₁ 2 ₁
Cell dimensions		
a, b, c (Å)	208.9, 379.4, 734.9	208.8, 378.5, 739.2
α, β, γ (°)	90, 90, 90	90, 90, 90
Resolution (Å)	200-3.47	200-4.9 (200-3.5)
R _{merge}	14.5	14.8
I / σ I	7.4	8.8
Completeness (%)	92.3	92.6 (57)
No.reflections	693,093	539,522
Redundancy	6.2	8.8
Overall σ_2	1.5	1.5
 <u>Refinement</u>		
Resolution (Å)	70-3.5	
R _{work} /R _{free}	29/34.9	

Table 4: Diffraction statistics for the *E.coli* 70S ribosome crystals in complex with ecRRF and ttRRF

	70S-ecRRF	70S-ttRRF
Data collection		
Space group	P2 ₁ 2 ₁ 2 ₁	P2 ₁ 2 ₁ 2 ₁
Cell dimensions		
a, b, c (Å)	210, 378, 737.1	209.9, 377.5, 737.6
α, β, γ (°)	90, 90, 90	90, 90, 90
Resolution (Å)	200-8	200-8 (200-4.5)
R _{merge}	15.8	8.5
I / σ I	8.4	5.2
Completeness (%)	100	95 (64)
No.reflections	102,519	372,460
Redundancy	6.2	10.1
Overall σ_2	1.1	0.76